



CHORUS

This is the accepted manuscript made available via CHORUS. The article has been published as:

Evidence for the constancy of U in the Mott transition of $V_{2}O_{3}$

H. Fujiwara, A. Sekiyama, S.-K. Mo, J. W. Allen, J. Yamaguchi, G. Funabashi, S. Imada, P. Metcalf, A. Higashiya, M. Yabashi, K. Tamasaku, T. Ishikawa, and S. Suga

Phys. Rev. B **84**, 075117 — Published 8 August 2011

DOI: [10.1103/PhysRevB.84.075117](https://doi.org/10.1103/PhysRevB.84.075117)

Evidence for the constancy of U in the Mott transition of V_2O_3

H. Fujiwara,^{1,2} A. Sekiyama,^{1,3} S.-K. Mo,^{4,5} J. W. Allen,⁴ J. Yamaguchi,¹ G. Funabashi,¹ S. Imada,¹ P. Metcalf,⁶ A. Higashiya,³ M. Yabashi,^{3,7} K. Tamasaku,³ T. Ishikawa,³ and S. Suga^{1,3}

¹Graduate School of Engineering Science, Osaka University, Toyonaka, Osaka 560-8531, Japan

²II. Physikalisches Institut, Universität zu Köln, Zùlpicher Straße 77, 50937 Köln, Germany

³SPRING-8/RIKEN, Kouto 1-1-1, Sayo, Hyogo 679-5148, Japan

⁴Randall Laboratory of Physics, University of Michigan, Ann Arbor, Michigan 48109, USA

⁵Department of Physics, Stanford University, Stanford, California 94305, USA

⁶Department of Physics, Purdue University, West Lafayette, Indiana 47907, USA

⁷SPRING-8/JASRI, Kouto 1-1-1, Sayo, Hyogo 679-5198, Japan

(Dated: June 16, 2011)

We have performed high-resolution hard X-ray photoemission spectroscopy for the metal-insulator transition (MIT) system $(V_{1-x}Cr_x)_2O_3$ in the paramagnetic metal, paramagnetic insulator and antiferromagnetic insulator phases. The quality of the spectra enables us to conclude that the on-site Coulomb energy U does not change through the MIT, which eliminates all but one theoretical MIT scenario in this paradigm material.

PACS numbers: 71.30.+h, 71.27.+a, 79.60.-i

I. INTRODUCTION

The Mott-Hubbard metal-insulator transition (MH-MIT) is a fundamental phenomenon not only for strongly correlated physics¹ but also for solid state physics generally. Dynamical mean field theory (DMFT)² has provided a new conceptual framework for describing how the MH-MIT occurs in the one-band Hubbard model when the on-site Coulomb repulsion U exceeds a critical value U_c relative to the inter-site hopping energy W . Nonetheless, even when DMFT is combined with realistic electronic structure calculations in the local density approximation (LDA+DMFT), an internally consistent description of the MIT *as it is observed in nature* has not yet emerged. This is true even for the most heavily studied paradigmatic material V_2O_3 . This material shows a first order transition from a high-temperature paramagnetic metal (PM) phase to a low-temperature antiferromagnetic insulator (AFI) phase at $T_N \approx 155$ K, accompanied by a structural change from the corundum phase to the monoclinic phase³⁻⁵. Slight Cr-substitution on the V sites develops a paramagnetic insulator (PI) phase with the same corundum structure above $T_N \approx 180$ K as shown in the inset of Fig. 1. In the comparison between early LDA+DMFT calculations⁶⁻⁹ and valence band photoemission spectra, the U value consistent with spectroscopy¹⁰ is too small to allow the MIT for the W values found in the LDA calculations for the various phases.

This basic tension concerning U has proved to be continuing and pervasive even though the theory has been made more sophisticated. Since changes in the V $3d$ orbital occupation are reported through all these transitions¹¹, an interplay among the spin-, charge- and orbital-degrees of freedom is thought to be essential for MIT. More recent LDA + DMFT studies suggest that an effective trigonal crystal field splitting leads to a redistribution of the orbital populations (known as the orbital selective MIT)^{12,13}. Nonetheless U must still be changed through the transition in the cited theories. A very interesting alternative concept is that the orbital polarization induced by a slight enhancement of the effective crystal field splitting can reduce U_c/W and thereby facilitate the MIT^{14,15} even though U is unchanged. Thus there are now only two possibilities on the table for V_2O_3 , either U or U_c changes in the MIT. A direct experimental determination of the differences in the bulk electronic structures and the value of U in all three phases is essential to move the issue forward.

In this paper, we report a state of the art hard X-ray photoemission spectroscopy (HAXPES) study to tackle this problem. Since U/W is known to be much different for the surface and the bulk, bulk sensitive HAXPES with $h\nu = 5 - 8$ keV¹⁶⁻²⁰ is essential by virtue of its large probing depth (> 50 Å at $h\nu \sim 8$ keV). The very high quality of our HAXPES spectra relative to that of earlier studies enables a detailed analysis to identify in all three phases the incoherent part of the V $3d$ spectrum, i.e. the lower Hubbard band (LHB) that defines U on the photoemission side of the Fermi level E_F . Thereby we obtain very strong evidence that U stays essentially constant through the MIT in $(V_{1-x}Cr_x)_2O_3$, leaving a change in U_c/W as the viable scenario for the MIT.

II. EXPERIMENT

HAXPES was performed at BL19LXU in SPring-8 with use of an MBS A1-HE hemispherical analyzer system. The linearly polarized light at ~ 8 keV was delivered from an in-vacuum 27-m long undulator²¹. The beam was focused onto the sample within $50 \times 100 \mu\text{m}^2$. The overall energy resolution was set to 220 meV for the wide scan of the valence band and 130 meV for the high-resolution mode near E_F as confirmed by the Au Fermi-edge. Well-annealed oriented single crystalline samples were cleaved *in situ* in a vacuum of 8×10^{-8} Pa. The measurement was performed above and below the temperatures of the PM-AFI and PI-AFI transitions (inset of Fig. 1). Soft X-ray photoemission spectroscopy (SXPES) measurements were carried out at BL25SU in SPring-8 with a comparable energy resolution^{7,9}.

III. RESULTS AND DISCUSSION

Figure 1 shows the HAXPES spectra of $(V_{1-x}Cr_x)_2O_3$ ($x = 0$ and 0.015) of the entire valence band. A Shirley-type inelastic integral background is subtracted from each spectrum and the spectra are normalized by their integrated area over the whole energy range of the valence band in all phases. In Fig 1, one can recognize that the AFI spectra of the samples with and without Cr-doping are very similar to each other, demonstrating the negligible effect of disorder on the electronic structure. All phases show a large peak structure around -8 eV, which is derived from O $2p$ states hybridized with V $4s$ and $3d$ states²².

Figure 2 displays the high-resolution HAXPES spectra reflecting the bulk V $3d$ electronic states. The background is subtracted in the same manner as for Fig. 1. It is useful to first compare the PM and PI spectra (Fig. 2(b)), for which the problem is simplified by excluding the roles of both the magnetic long-range ordering and the structural phase transition. The PM spectrum in Fig. 2(b) shows the prominent quasiparticle (QP) peak just below E_F . In addition, the small bump structure observed around -1.3 eV is ascribed to the incoherent part corresponding to the LHB^{7,9,19}. In contrast the PI spectrum shows a gap opening, with a strong spectral weight transfer across the PM-PI transition.

A strong spectral weight transfer is also observed across the PM-AFI transition as shown in the Fig 2(a), indicating that the crystal symmetry change in this transition is not a major factor of the MIT in $(V_{1-x}Cr_x)_2O_3$. There are however noticeable differences in the AFI and PI lineshapes. First the AFI phase band gap is larger (220 meV from E_F) and the threshold is noticeably sharper than for the PI phase (Figs. 2(a) and (b)), in agreement with the results of optical measurements²³ and the previous SXPES⁹. These differences are seen directly in the spectra for the PI-AFI transition shown in Fig. 2(c) and also in the negative and positive peaks in the regions near -0.25 and $-0.5 \sim -0.85$ eV in the difference spectrum in Fig. 2(d). Second the spectra in both the doped and undoped AFI phases clearly consist of multi-components as indicated by the two vertical bars for the shoulder and peak structures at around -1.3 and -0.5 eV, respectively (Fig. 2(a)). The AFI structure at -1.3 eV can most likely be ascribed to the LHB. On the other hand, the -0.5 eV peak was not predicted by the early LDA+DMFT calculations for V_2O_3 ⁶. Most interesting is that the LHB energy position seems to be not different in all three phases as indicated by shaded bars in Fig. 2. We further notice in Fig. 2(c) that the tails on the lower energy side (from -2 to -3 eV) are almost identical, suggesting that U (as observed on the PES side of E_F) may be essentially the same in these two phases. In order to confirm this conclusion, it is essential to know the energy positions of the LHB in all phases. To do that we must first establish firmly the origin of the -0.5 eV peak in the AFI phase.

In Figs. 3(a), (b) and (c), we show the $h\nu$ dependences of the spectral weight near E_F for all three phases. For easy comparison of the intensity near E_F , the background is here subtracted in the same manner as in refs.7,9 and the spectra are normalized below -1 eV. As shown in Fig. 3(a) for the PM phase, the relative weight between E_F and -1 eV representing the QP-peak increases remarkably with increasing $h\nu$ from 60 eV²⁴ to 8180 eV in the PM phase. This development of the QP-peak is not due to a change of the relative cross-sections of V $3d$ and O $2p$ states, but to the enhancement of the bulk contribution in accordance with the increase of the probing depth^{7,9}. We also show that the extracted bulk component from the photoemission spectra at $h\nu = 700$ and 60 eV^{7,25} is in full agreement with the HAXPES spectrum. Thus the increase of the relative intensity of the QP-peak can be interpreted as due to the reduction of the U/W in the bulk caused by the wider bandwidth W in the bulk than in the surface. We note in passing that the finding of a larger QP peak in the HAXPES spectrum demands a smaller value of U , which exacerbates the problem that U is then too small to enable the MIT.

The structure near -0.5 eV in the AFI and PI phases increases also with increasing $h\nu$, as seen very clearly in Figs. 3(b) and (c), even though the difference between $h\nu = 8$ keV and 700 eV is smaller than for the PM phase, reflecting a smaller difference between the bulk and surface in the AFI and PI phases. Although the presence of this spectral feature in the AFI phase has been inferred in the previous study⁹, it is here much more clearly seen by its extraction from SXPES spectra at 700 and 220 eV. The extracted spectrum is fully consistent with the directly detected spectrum by bulk sensitive HAXPES. Following the early suggestion by Rozenberg *et al.*²⁷, the increase

of the structure near -0.5 eV in the AFI phase can be ascribed²⁸ to a QP induced by long-range spin coherence. The statistics of the PI phase HAXPES spectrum are slightly worse than for the AFI phase but the extracted bulk spectrum in Fig. 3(c) demonstrates clearly a difference between the surface and bulk electronic structures even in the PI phase. The observable increase of the bulk PES intensity with $h\nu$ may be ascribed to “residual” spectral weight resulting from the short range magnetic order detected by neutron scattering²⁹ in the PI phase. The slight transfer of the spectral weight across the PI-AFI transition as seen in Fig. 2(c) and Fig. 3(d) can now be understood as due to the switching from the short range magnetic order to the long range ordering.

We now proceed to identify the LHB in the AFI spectrum. For this we have adopted as a working hypothesis that for the resolution of the experiment the QP component in the AFI phase has essentially the same spectral shape as in the PM phase. We shift the PM spectrum and normalize it to realize a good fit to the leading edge of the AFI spectrum as shown by the thin solid curve in Fig. 3(e). Then this spectral shape is subtracted from the AFI spectrum, yielding the LHB in the AFI phase as shown by the thick solid curve in Fig. 3(f). The peak position of the LHB in the AFI phase indicated by the vertical bar is thus estimated as -1.2 ± 0.15 eV, which is almost degenerate with that of the PM phase.

In order to test the robustness of the evaluation of the LHB position, we further explore the sensitivity of the result to two possible corrections to our subtraction procedure. First, our procedure may have subtracted too much weight from the AFI LHB region because the LHB of the PM spectrum is also subtracted. To test the importance of this effect we have repeated the procedure but with an alternate subtracted lineshape having only a smooth tail extending to higher energy from the PM phase QP-peak, as shown by the thin solid line labeled gtype 2h in Fig. 4(a). The resulting LHB is shown as the thick solid curve in Fig. 4(b)). The subtraction procedure in Fig. 3 (e) and (f) corresponds to the case labeled gtype 1h in Fig. 4(a) and (b). The position of the AFI phase LHB is seen to be robust against this first correction, i.e. still degenerate in energy with the PI phase LHB. Second, one may think of the possibility that the peak of the coherent component in the AFI phase overlaps with the QP peak in the PM spectra. To check this possibility, we fit the type 2 lineshape of Fig. 4(a) at the very top of the leading edge peak as shown in Fig. 4(c). The resulting LHB is the solid curve in Fig. 4(d) and its position is again degenerate with the LHB of the PM spectra. Thus the energy position of the AFI LHB is robust against these possible variations of the QP peak extraction procedure. Even if the LHB in the PM phase is not subtracted from the AFI spectrum, no essential change is seen for the LHB spectral weight in the AFI phase. More extremely, accounting for a possible overlap of the AFI and PM phase coherent peaks also does not change the LHB position, so the possibility that the LHB in the AFI phase is deeper than that in PM phase is definitely excluded.

We note that the position of the LHB peak is also robust for the photon energy dependence of the valence band spectra, and thereby it does not change between the surface and the bulk as shown in Fig. 3(a), (b), (c), and the previous reports^{7,30}. U is defined by the separation of the LHB and the upper Hubbard band (UHB) on the unoccupied side of E_F , which we do not observe. However, if U increases in the insulating phases due to a reduction in screening, it is highly unlikely that the UHB can shift while the LHB remains fixed. Therefore we conclude that U stays essentially constant through the MIT in $(V_{1-x}Cr_x)_2O_3$.

Our result strongly supports the scenario^{14,15} of the orbital selective Mott-transition in which U_c/W changes through the MIT due to the enhancement of the effective trigonal crystal field splitting. We remark that this idea is also supported by the observation in an optical study³¹ long ago of uniaxial stress-induced spin flop in Cr_2O_3 . Considering the stress dependences of Cr^{3+} states in ruby³², the spin flop mechanism could be traced to a sign change in the magnetocrystalline anisotropy, driven primarily by a change in the trigonal crystal field. One infers that the trigonal splitting is very strain sensitive in this crystal structure, which may well be the key to making a unified explanation of the MIT in $(V_{1-x}Cr_x)_2O_3$, i.e. U is consistent with the PM phase QP weight and unchanging through the transition, W has changing values as found in LDA, and the MIT is enabled for these values of fixed U and changing W by a changing value of U_c .

IV. CONCLUSION

In conclusion, the high resolution HAXPES gives noticeable spectral weight transfers for the bulk electronic states in $(V_{1-x}Cr_x)_2O_3$ ($x = 0, 0.015$) across all three phase transitions. The QP-peak of the AFI phase due to the long-range magnetic ordering is clearly observed and enables an identification of LHB. The essentially degenerate LHB for all three phases yields strong evidence that U stays constant through the MIT. This finding renders a changing U_c/W in an orbital selective Mott-transition as currently the only viable scenario for the MIT in $(V_{1-x}Cr_x)_2O_3$. An understanding of the MIT as it is observed in nature for a paradigm material may finally be at hand.

V. ACKNOWLEDGMENTS

We thank L. H. Tjeng, I. Nekrasov, K. Haule, and G. Kotliar for fruitful discussions. We express appreciation to S. Komori, M. Obara, Y. Nakatsu, Y. Tomida and M. Y. Kimura for supporting the measurements. This work was supported in part by a Grant-in-Aid for Global COE (G10), Innovative Areas "Heavy Electrons" (20102003), and Scientific Research (18104007, 18684015, 21740229, and 21340101) from MEXT and JSPS, Japan. Work at UM was supported by the U.S. DOE under Contract No. DE-FG02-07ER46379. SKM is funded by US NSF. HF thanks the Alexander von Humboldt Foundation for their support. SXPES was performed under the approval of the Japan Synchrotron Radiation Research Institute (2006B1722,2009B1014).

-
- ¹ M. Imada, A. Fujimori, Y. Tokura, Rev. Mod. Phys. **70**, 1039 (1998).
- ² A. Georges, G. Kotliar, W. Krauth, M. J. Rozenberg, Rev. Mod. Phys. **68**, 13 (1996).
- ³ D. B. McWhan, T. M. Rice, and J. P. Remeika, Phys. Rev. Lett. **23**, 1384 (1969).
- ⁴ P. D. Dernier, J. Phys. Chem. Solids **31** 2569 (1970).
- ⁵ R. M. Moon, Phys. Rev. Lett. **25**, 527 (1970).
- ⁶ K. Held, G. Keller, V. Eyert, D. Vollhardt, and V. I. Anisimov, Phys. Rev. Lett. **86**, 5345 (2001).
- ⁷ S.-K. Mo, J. D. Denlinger, H.-D. Kim, J.-H. Park, J. W. Allen, A. Sekiyama, A. Yamasaki, K. Kadono, S. Suga, Y. Saitoh, T. Muro, P. Metcalf, G. Keller, K. Held, V. Eyert, V. I. Anisimov, and D. Vollhardt, Phys. Rev. Lett. **90**, 186403 (2003).
- ⁸ G. Keller, K. Held, V. Eyert, D. Vollhardt, and V. I. Anisimov, Phys. Rev. B **70**, 205116 (2004).
- ⁹ S.-K. Mo, H.-D. Kim, J. D. Denlinger, J. W. Allen, J.-H. Park, A. Sekiyama, A. Yamasaki, S. Suga, Y. Saitoh, T. Muro, and P. Metcalf, Phys. Rev. B **74**, 165101 (2006).
- ¹⁰ Of greatest quantitative significance are the relative weights of the two V 3d spectral features discussed in this paper, the quasiparticle peak and the incoherent part.
- ¹¹ J.-H. Park, L. H. Tjeng, A. Tanaka, J. W. Allen, C. T. Chen, P. Metcalf, J. M. Honig, F. M. F. de Groot and G. A. Sawatzky, Phys. Rev. B **61**, 11506 (2000).
- ¹² M. S. Laad, L. Craco and E. Müller-Hartmann, Phys. Rev. B **73**, 045109 (2006).
- ¹³ A. I. Poteryaev, J. M. Tomczak, S. Biermann, A. Georges, A. I. Lichtenstein, A. N. Rubtsov, T. Saha-Dasgupta, and O. K. Andersen, Phys. Rev. B **76**, 085127 (2007).
- ¹⁴ E. Pavarini, S. Biermann, A. Poteryaev, A. I. Lichtenstein, A. Georges, and O. K. Andersen, Phys. Rev. Lett. **92**, 176403 (2004).
- ¹⁵ A. I. Poteryaev, M. Ferrero, A. Georges, O. Parcollet, Phys. Rev. B **78**, 045115 (2008)
- ¹⁶ N. Kamakura, M. Taguchi, A. Chainani, Y. Takata, K. Horiba, K. Yamamoto, K. Tamasaku, Y. Nishino, D. Miwa, E. Ikenaga, M. Awaji, A. Takeuchi, H. Ohashi, Y. Senba, H. Namatame, M. Taniguchi, T. Ishikawa, K. Kobayashi and S. Shin, Europhys. Lett. **68**, 557 (2004).
- ¹⁷ M. Taguchi, A. Chainani, N. Kamakura, K. Horiba, Y. Takata, M. Yabashi, K. Tamasaku, Y. Nishino, D. Miwa, T. Ishikawa, S. Shin, E. Ikenaga, T. Yokoya, K. Kobayashi, T. Mochiku, K. Hirata, and K. Motoya, Phys. Rev. B **71**, 155102 (2005).
- ¹⁸ S. Suga, A. Sekiyama, S. Imada, A. Shigemoto, A. Yamasaki, M. Tsunekawa, C. Dallera, L. Braicovich, T.-L. Lee, O. Sakai, T. Ebihara and Y. Önuki, J. Phys. Soc. Jpn **74**, 2880 (2005).
- ¹⁹ G. Panaccione, M. Altarelli, A. Fondacaro, A. Georges, S. Huotari, P. Lacovig, A. Lichtenstein, P. Metcalf, G. Monaco, F. Offi, L. Paolasini, A. Poteryaev, O. Tjernberg, and M. Sacchi, Phys. Rev. Lett. **97**, 116401 (2006).
- ²⁰ A. Yamasaki, S. Imada, H. Higashimichi, H. Fujiwara, T. Saita, T. Miyamachi, A. Sekiyama, H. Sugawara, D. Kikuchi, H. Sato, A. Higashiya, M. Yabashi, K. Tamasaku, D. Miwa, T. Ishikawa, and S. Suga, Phys. Rev. Lett. **98**, 156402 (2007).
- ²¹ M. Yabashi, K. Tamasaku, and T. Ishikawa, Phys. Rev. Lett. **87**, 140801 (2001).
- ²² J. C. Woicik, M. Yekutieli, E. J. Nelson, N. Jacobson, P. Pfalzer, M. Klemm, S. Horn, and L. Kronik, Phys. Rev. B **76**, 165101 (2007) ; T. C. Koethe and L. H. Tjeng, preprint; A. Sekiyama *et al.*, unpublished; E. Papalazarou, Matteo Gatti, M. Marsi, V. Brouet, F. Iori, Lucia Reining, E. Annese, I. Vobornik, F. Offi, A. Fondacaro, S. Huotari, P. Lacovig, O. Tjernberg, N. B. Brookes, M. Sacchi, P. Metcalf and G. Panaccione, Phys. Rev. B **80**, 155115 (2009)
- ²³ A. S. Barker *et al.*, Solid State Communications **8**, 1521(1970); G. A. Thomas *et al.*, Phys. Rev. Lett. **73**, 1529 (1994).
- ²⁴ M. Schramme, *thesis*, Universität Augsburg, (2000).
- ²⁵ The PES spectrum can be written as the linear combination of the bulk and surface spectral weight. The bulk and surface emission ratio I_s/I_b is given by $I_s/I_b = \exp(d/\lambda \cos\theta) - 1$, where d is surface layer thickness (2.44 Å) and λ is the electron escape depth²⁶. Detail description is written in Ref.⁹.
- ²⁶ A. Tanuma, C. J. Powell, and D. R. Penn, Surf. Sci. **192**, L849 (1987).
- ²⁷ M. J. Rozenberg, G. Kotliar, and H. Kajueter, Phys. Rev. B **54**, 8452 (1996).
- ²⁸ G. Sangiovanni, A. Toschi, E. Koch, K. Held, M. Capone, C. Castellani, O. Gunnarsson, S.-K. Mo, J. W. Allen, H.-D. Kim, A. Sekiyama, A. Yamasaki, S. Suga, and P. Metcalf, Phys. Rev. B **73**, 205121 (2006).
- ²⁹ W. Bao, C. Broholm, G. Aeppli, P. Dai, J. M. Honig, and P. Metcalf, Phys. Rev. Lett. **78**, 507 (1997).
- ³⁰ A. Sekiyama, H. Fujiwara, S. Imada, S. Suga, H. Eisaki, S. I. Uchida, K. Takegahara, H. Harima, Y. Saitoh, I. A. Nekrasov, G. Keller, D. E. Kondakov, A.V. Kozhevnikov, Th. Pruschke, K. Held, D. Vollhardt, and V. I. Anisimov, Phys. Rev. Lett. **93**, 156402 (2004).
- ³¹ J. W. Allen, Phys. Rev. Lett. **27**, 1526 (1971)
- ³² E. Feher and M. D. Sturge, Phys. Rev. **172**, 244 (1968)

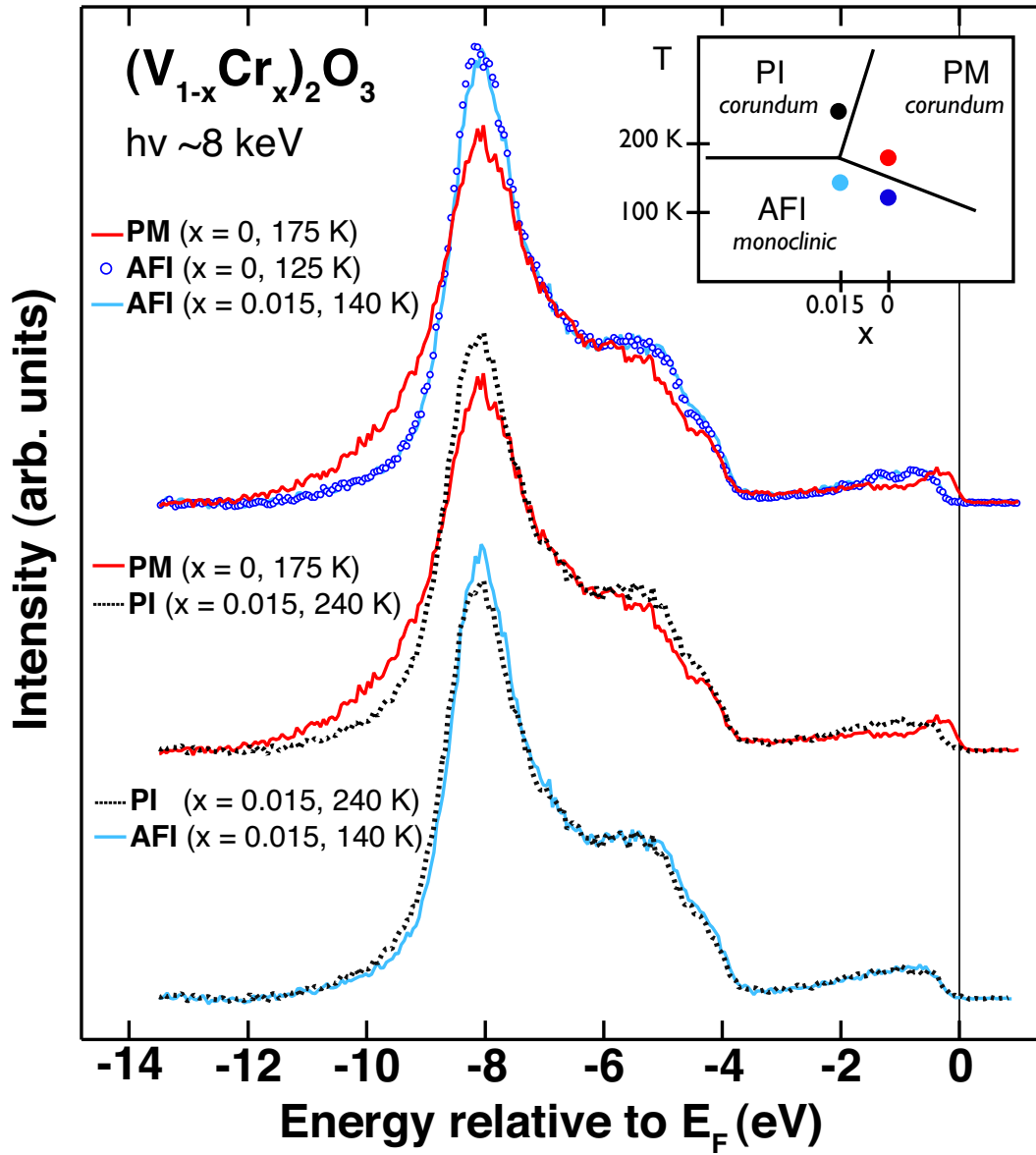


FIG. 1: (color online). Entire valence band spectra of $(V_{1-x}Cr_x)_2O_3$ ($x = 0$ and 0.015) in the PM and AFI phases (top), those in the PM and PI phases (middle), and those in the PI and AFI phases (bottom). Inset shows the schematic phase diagram of $(V_{1-x}Cr_x)_2O_3$.

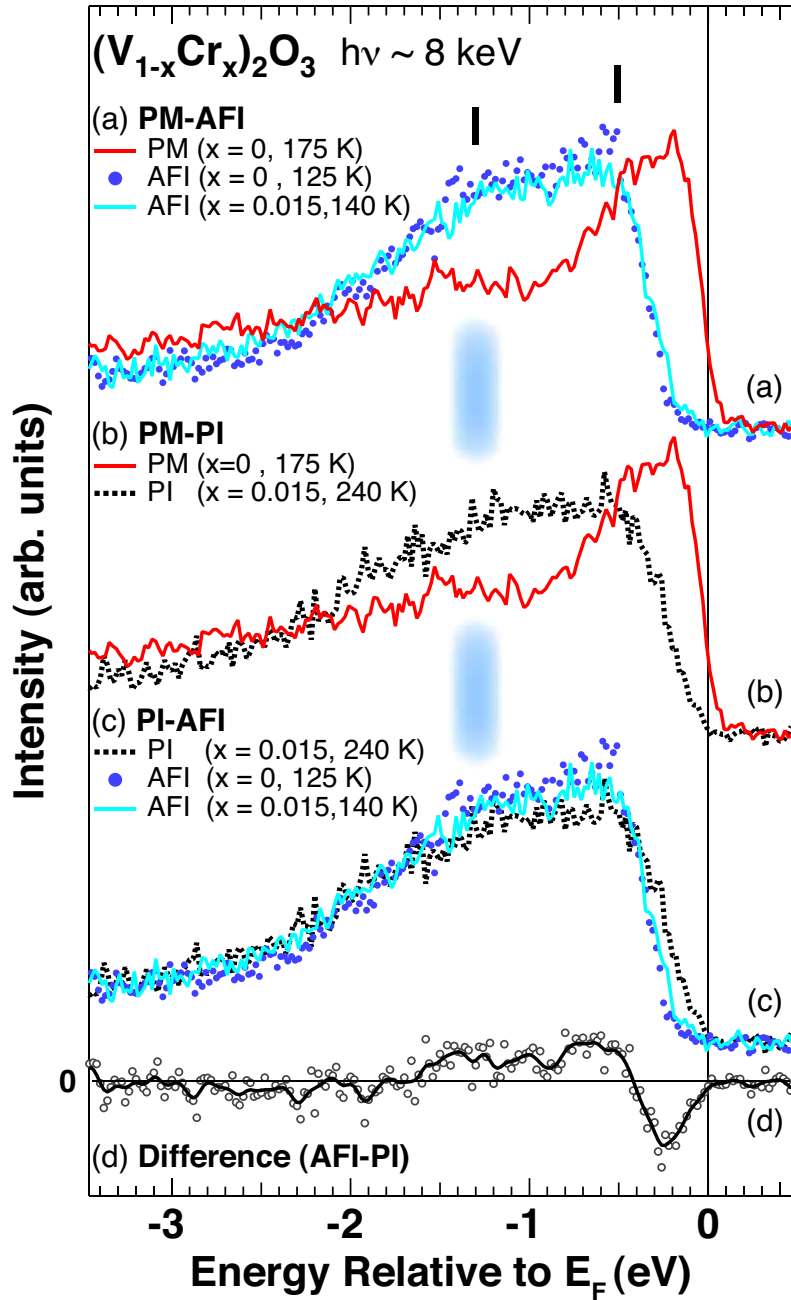


FIG. 2: (color online). High-resolution HAXPES spectra of $(V_{1-x}Cr_x)_2O_3$ ($x = 0$ and 0.015) near E_F in the PM and AFI phases (a), those in the PM and PI phases (b), and those in the PI and AFI phases (c). (d) The difference between the AFI and PI spectra (open circle), which is estimated by averaging the two results for the $x = 0$ and 0.015 AFI spectra. The thick solid line is the smoothed difference.

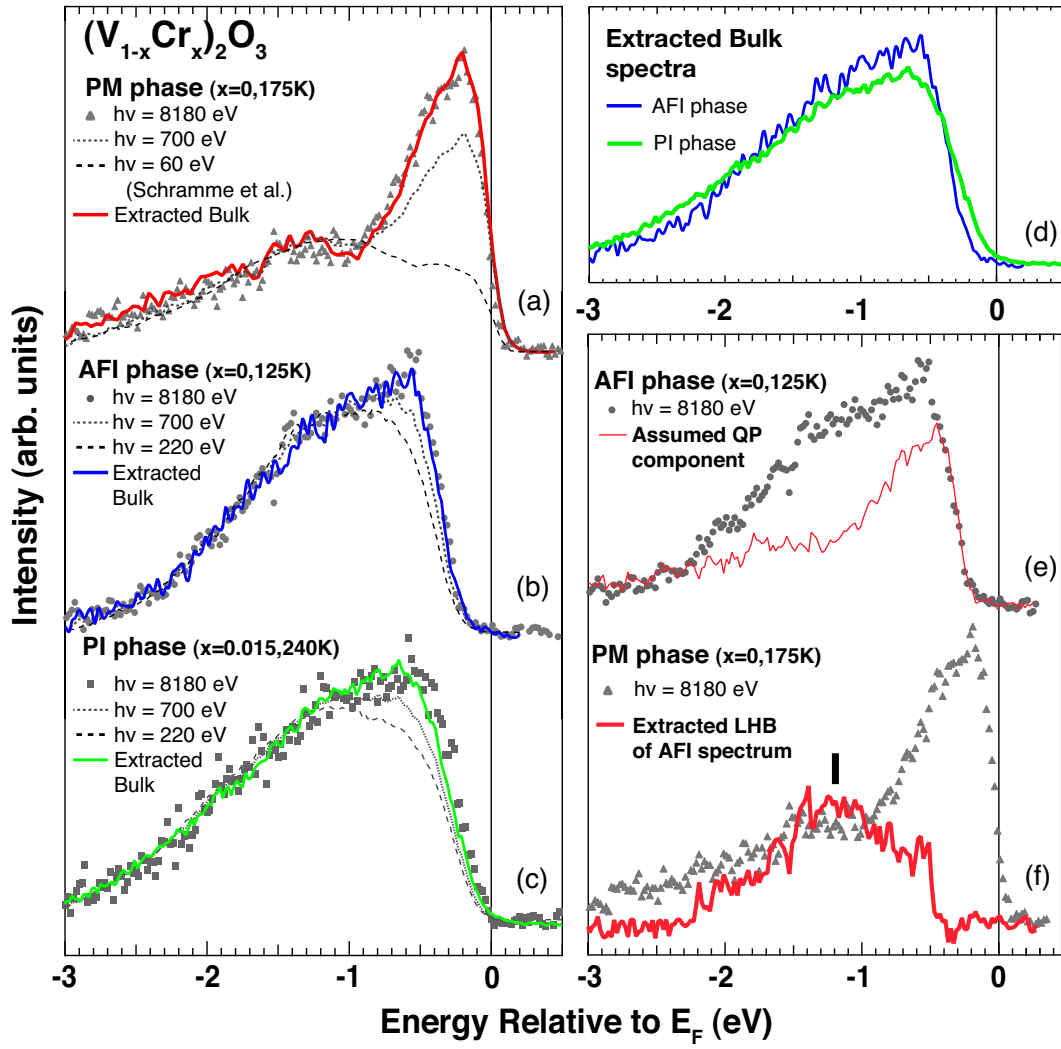


FIG. 3: (color online). (left panel) Photon energy dependence of the V 3d spectral weight near E_F for V_2O_3 taken by HAXPES and SXPES in the PM phase (a), AFI phase (b), PI phase (c). Solid lines in (a), (b) and (c) show the bulk component extracted from the PES spectra taken at 700 and 60 eV²⁴ (700 and 220 eV) photons in the PM (AFI and PI) phase. (right panel) Comparison of the extracted bulk spectra between AFI and PI phases after normalization by the integrated intensity (d). In (e) and (f), the extracted LHB of AFI phase is evaluated by the procedure mentioned in the text in detail.

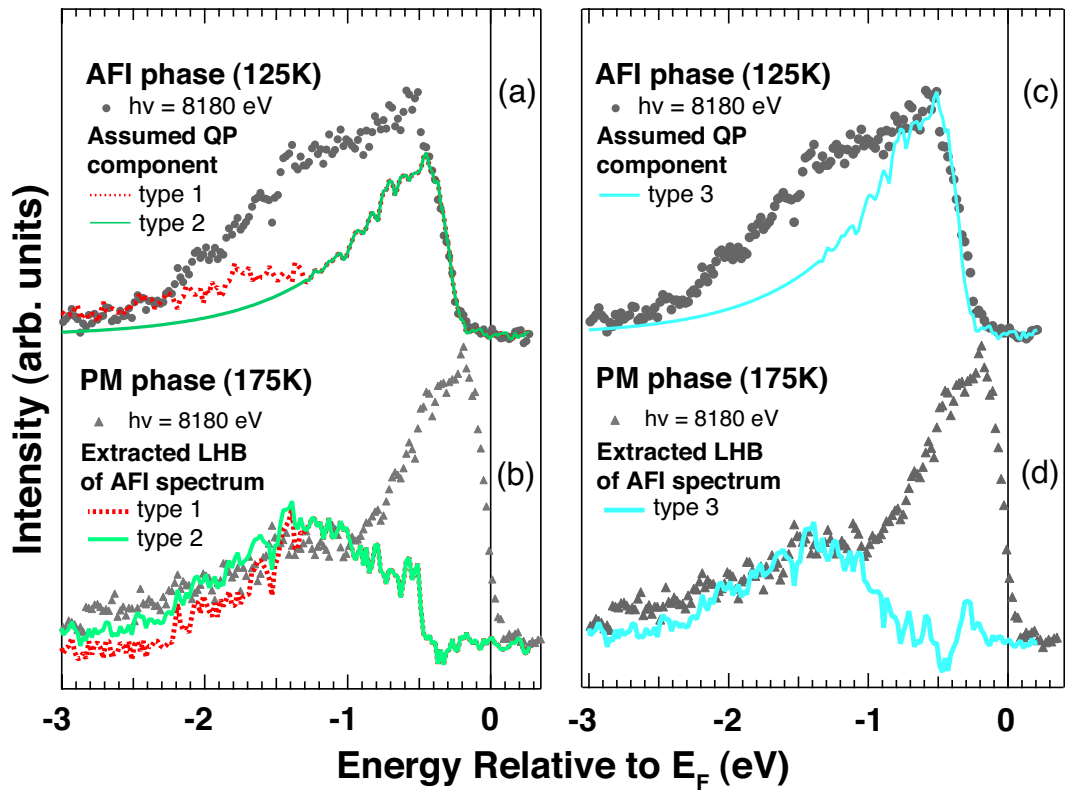


FIG. 4: (color online). Comparison of the extracted LHB of AFI phase evaluated by the three types of the subtraction procedures mentioned in the text in detail.